COMPARATIVE ASSESSMENT OF THE INTERLAYER SHEAR-BOND STRENGTH OF GEOGRID REINFORCEMENTS IN HOT-MIX ASPHALT

Lubinda F. Walubita
Research Scientist & Professor (Adjunct)
TTI – The Texas A&M University System
College Station, TX 77843, USA | E-mail: lfwalubita@tamu.edu

Tito P. Nyamuhokya
Associate Transportation Researcher
TTI – The Texas A&M University System
College Station, TX 77843, USA | E-mail: t-nyamuhokya@tti.tamu.edu

Julius J. Komba
Senior Research Engineer
CSIR – Council for Scientific and Industrial Research /
Ph.D. Candidate, University of Pretoria
Pretoria, South Africa | E-mail: jkomba@csir.co.za

Hossain Ahmed Tanvir
Design Engineer II
Trendsetter Engineering Inc.
Houston, TX 77070, USA | Email: h.tanvir@trendsetterengineering.com

Mena I. Souliman, Corresponding Author
Assistant Professor
The University of Texas at Tyler, Department of Civil Engineering
Tyler, TX 75701, USA | E-mail: msouliman@uttyler.edu

Bhaven Naik
Assistant Professor
Ohio University
Athens, OH 45701, USA |Email: naik@ohio.edu

Highlights

- Evaluated impacts of geogrid on the HMA-overlays interlayer bond strength.
- Unreinforced, polyester (FA) and fiberglass (FG) based interlayers were assessed.
- The unreinforced HMA samples exhibited the highest bond strength followed by FA.
- The HMA samples with FG based geogrids exhibited the least bond strength.
- Geogrid type, size of mesh and strands both impacted the interlayer bond strength.

ABSTRACT

With the increasing use of geogrid reinforcements to mitigate reflective cracking in hot-mix asphalt (HMA) overlays, interlayer (interface) bonding has become an even more critical aspect of HMA placement/construction to mitigate delamination and debonding of the HMA overlay. To comparatively evaluate the interlayer bond strength due to the effects of the geogrid reinforcements, the shear bond strength test was conducted in this laboratory study, using unreinforced control HMA samples as the reference datum. Cylindrical HMA samples (150 mm diameter) gyratory compacted in two 75-mm lift thicknesses, with the geogrid reinforcement in-between the two lifts, were used for testing at room temperature under a monotonically shear loading rate of 5 mm/min. Emulsified asphalt was used as the interlayer tack coat and six different geogrid materials, which are polyester-based (FA) and fiberglass-based (FG), were comparatively evaluated. As theoretically expected, the control (unreinforced) HMA samples exhibited superiority followed closely by samples reinforced with polyester-based geogrids. Although comparable to the values reported in the literature, HMA samples reinforced with fiberglass-based geogrids performed the poorest with the lowest interlayer bond strengths – that is the polyester-based outperformed the fiberglass-based geogrids. Overall, the interlayer bond strength exhibited a general decreasing trend with a decrease in the geogrid mesh size (open area), increase in the geogrid strand thickness, and material grade. Thus, in as much as reflective crack mitigation is structurally desired, due diligence must be cautiously exercised when selecting the geogrid type/grade for use in HMA reinforcement to ensure sufficient interlayer bonding and minimize any potential delamination/debonding problems in service.

Keywords: Reflective Cracking, Geogrid, Fortgrid Asphalt (FA), Fiberglass (FG), Shear, Bond Strength

INTRODUCTION

One of the common maintenance/rehabilitation methods used to mitigate reflective cracking in old existing cracked pavements, be it flexible hot-mix asphalt (HMA) or concrete, is the structural application of crack-impeding and interlayer grid reinforcements. Quite often, these grid reinforcements are used as part of the HMA overlay construction in maintenance and/or rehabilitation projects because of their effectiveness in arresting reflective cracking and cost-effectively increasing the service life and longevity of HMA overlays (*1-8*). Figures 1 and 2 shows an example of an old cracked pavement and geogrid interlayer construction, respectively.

FIGURE 1 Example of an Old Cracked HMA Pavement.

FIGURE 2 Geogrid Interlayer Reinforcement and HMA Overlay Construction.

As shown in Figure 2, one of the fundamental functions of the interlayer grid reinforcement is to inhibit the upward propagation of cracks from an old existing cracked pavement to the surface, i.e., to mitigate the cracks from reflecting through the HMA overlay to the surface. Thereby, aiding in cost-effectively prolonging the cracking resistance and service life of the pavement (*8*).

Many types of interlayer grid reinforcement materials including geogrids, geotextiles, paving mats, paving fibers, etc., are presently available on the commercial market and widely used in HMA overlay projects during maintenance and rehabilitation activities (*9,10*). With the increasing use of these interlayer grid reinforcements, interlayer (interface) bonding becomes an even more critical aspect of HMA placement/construction to prevent delamination and debonding during service that could negatively impact the long-term performance, longevity, and durability of the overlay.

To comparatively evaluate the interlayer bond strength arising from the effects of the geogrid reinforcements, the shear bond strength test was conducted in this laboratory study, using unreinforced control HMA samples as the reference datum. Six different geogrid materials were comparatively evaluated for their corresponding interlayer shear bond strengths and are discussed in this paper.

In the subsequent section, a summation of the literature review findings on interlayer bond strength is presented. The experimental design plan for laboratory testing is subsequently presented followed by the laboratory test results, analysis, and synthesis of the findings. The paper then concludes with a summary of key findings and recommendations.

LITERATURE REVIEW

Based on the literature reviewed, there is currently no universally standardized test method or screening criteria for characterizing and quantifying the interlayer (interface) bond strength in HMA. Worldwide, many institutions, states, and countries appear to have their own standards and/or recommended bond strength values/limits that were determined based on different test methods and testing conditions (*11*). An example of some reviewed values from the literature is summarized in Table 1 and shows bond strength values ranging from as low as 100 kPa to as high as 1500 kPa for varying test methods/conditions. Based on field core testing, values ranging from 103 to 655 kPa have been measured with satisfactory in-service (field) interlayer bonding performance (*12*).

TABLE 1 Literature Review Results - HMA Interlayer Shear Bond Strength.

Reference Source	Institution/ State/Country	HMA Interlayer Bond Strength		Test /Comment
		Reported Values (kPa)	Recommendation	
(13)	MnDOT, USA	255-1379 (37-200 psi)	690 kPa	
(*14*)	NCHRP, USA	241-552 (35-80 psi)	276 kPa	Direct shear
(*15*)	NCAT, AL	483-1448 (70-210 psi)	600 kPa	Direct-shear, 25 °C
(*16*)	-	-	310 kPa	-
(*17*)	-	235-351	235 kPa	-
(*18*)	Jordan	150-740 (21-107 psi)	-	-
(*19*)	Canada	967 – 1298	-	Direct shear, 25 °C
(*20*)	South Africa	535-1184	400 kPa	Torque-based
(*12*)	Texas, USA	Lab = 276-1379 (40-200 psi) Field = 103-655 (15-95 psi)	-	Direct shear
(*21*)	FH, NZ	100-1200	275 kPa	Direct shear, 25-40 °C
(*22*)	NJ, USA	483-1103 (70-160 psi)	483 kPa	Direct shear
(11)	WV, USA	855-1500	-	Direct shear, 25 °C
(*23*)	VA, USA	1613-2124 (234-308 psi)	-	Torque-based

Most of the HMA bond strength tests reported in the literature are either direct-shear, tension, or torque-shear based. These include the interface-shear (PINE, ASTRA, etc), Leutner-shear, Superpave-shear, Limoges double-shear, layer-parallel direct shear, Pull-off, Arcan, A-tacker, Torque bond tests, etc. (*11, 12, 20, 21, 24*). As was used in this study, the direct-shear based tests have prominence due to their practicality, cost-effectiveness, repeatability, and ability to readily fit the already existing laboratory loading frames such as the Marshall stabilometer, universal testing machine (UTM), or material testing system (MTS).

Numerous studies have evaluated the various factors that influence the interlayer HMA bond-strength including mix-type, temperature, aggregate size, tack coat type, tack coat application rate, surface roughness, age, traffic, etc. (*11*, *14*, *15*, *21*,*25*–*30*). However, limited studies have specifically focused on the geogrid bond-strength effects. For instance, Tran et al. (*15*) reported that the interlayer bond strength generally improved with rougher milled surfaces than non-milled surfaces. By contrast, West et al. (*24*) and Al-Qadi et al. (*31*) observed a declining bond strength with an increase in temperature. However, the majority of these studies have been predominantly based on unreinforced HMA with or without tack coat – but, without any interlayer geogrid reinforcements in the HMA. Thus, the contribution of this study is primarily on evaluating the effects of the interlayer geogrid reinforcement on the bond strength in HMA, i.e., *What is the effect on the interlayer bond strength with the addition of geogrid reinforcements in HMA?* Whilst the interface bond can be measured, characterized, and quantified in terms of strength, modulus (stiffness), or work (energy), the monotonic shear bond strength parameter was used in this study (*21*).

LABORATORY TEST PLAN

Six different geogrid interlayer materials, which are a polyester-based coated with bitumen copolymer (fortgrid asphalt denoted as FA) and fiberglass-based (denoted as FG), were arbitrary selected and comparatively evaluated. As listed in Table 2, three FA and two FG material grades were evaluated against unreinforced HMA samples. The key characteristic differences and geometrical attributes as related to the interlayer bonding properties of the geogrids are also included in Table 2 along with pictorial illustrations in Figure 3. More technical details and other index properties of the individual geogrid materials can be found elsewhere (*9*).

TABLE 2 Geogrid Materials.

Geogrid	**Mesh View**	**Aperture (Mesh Opening) L × W = Area (mm^2)**	**Strand Thickness (mm)**	**Strand Width (mm)**	**%age HMA-HMA Contact over 150-mm diameter Area**
FA-30		28.3 × 28.3 ≈ 801	~0.63	~7.15	64%
FA-50		27.3 × 27.3 ≈ 743	~0.88	~9.15	54%
FA-75		25.5 × 25.5 ≈651	~1.01	~11.01	45%
FA-100		22.5 × 22.5 ≈ 507	~1.15	~12.65	42%
FG-50		21.4 × 21.4 ≈ 457	~0.55	~5.11	67%
FA-100	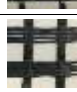	15.9 × 15.9 ≈ 253	~1.15	~11.01	40%
Control	-	-	-	-	100%

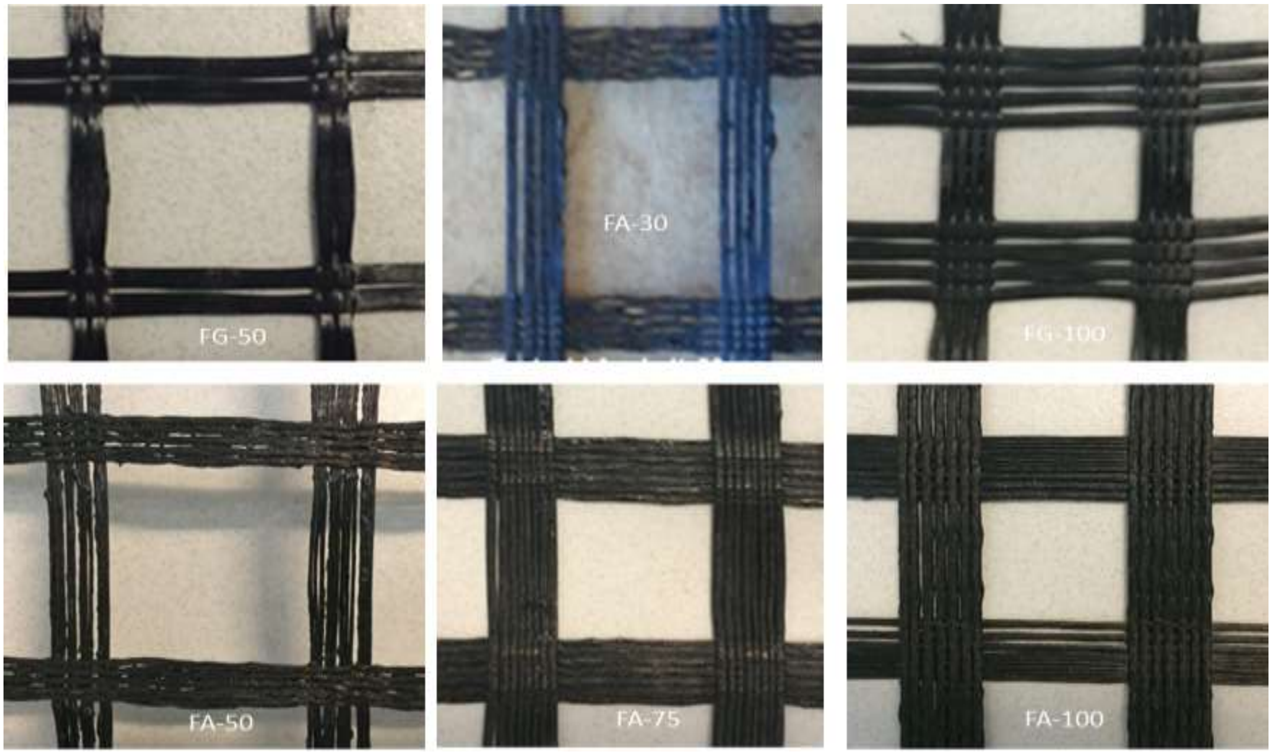

FIGURE 3 Pictorial Illustration of the Geogrid Materials.

HMA Mix and Sample Fabrication

A typical dense-graded 12.5 mm Nominal Maximum Aggregate Size (NMAS) mix, with limestone/dolomite/granite aggregates and 4.5% PG 64-22 asphalt-binder, was used. As illustrated in Table 3 and Figure 4, HMA cylindrical samples (150 mm diameter) were compacted in two 75-mm lift thicknesses using the Superpave gyratory compactor (SGC) – with the geogrid reinforcement in-between the two lifts, except for the control (unreinforced) HMA samples.

TABLE 3 HMA Sample Molding and Compaction Process.

#	HMA Sample (150-mm diameter)	Molding and Compaction Process
1	Control (unreinforced)	75-mm bottom lift + tack coat + 75-mm top lift = 150 mm total thickness
2	Geogrid reinforced	75-mm bottom lift + tack coat + *grid* + 75-mm top lift = 150 mm total thickness

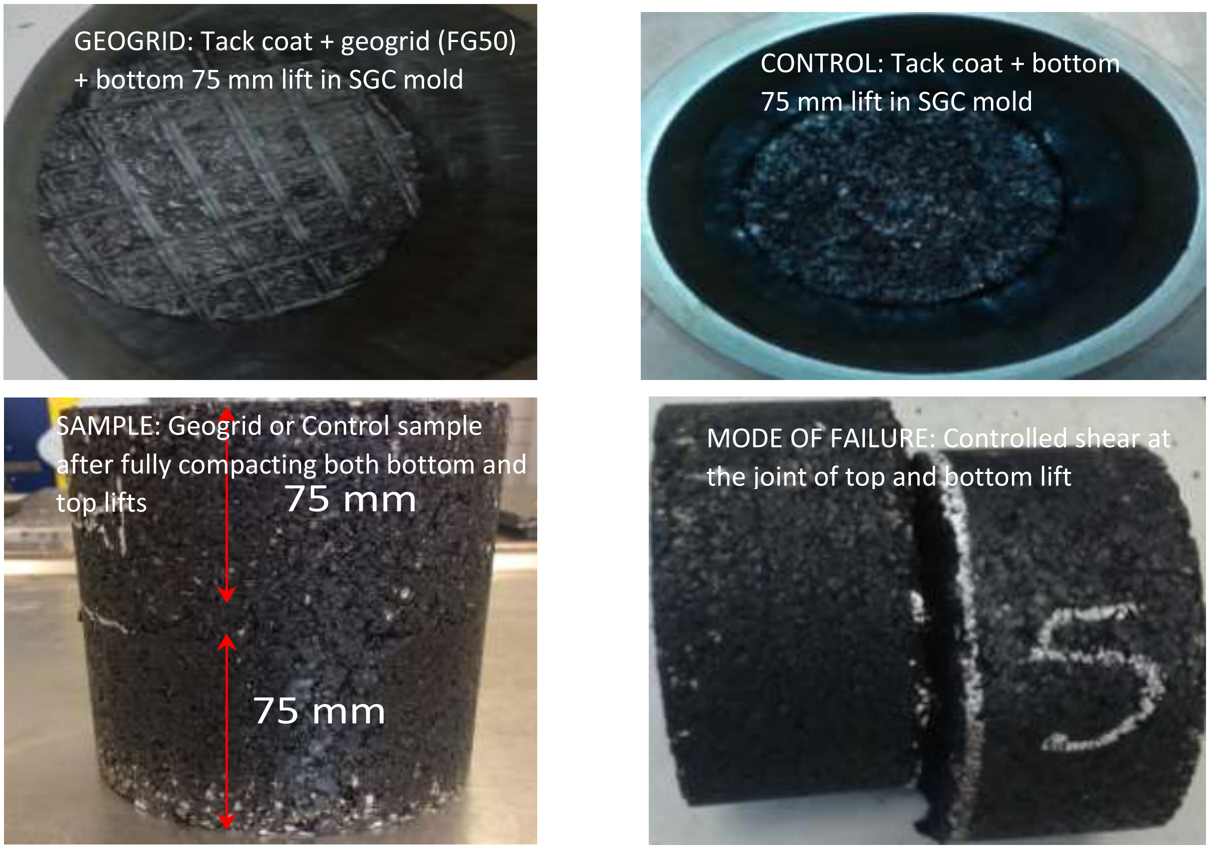

FIGURE 4 HMA Sample Fabrication and Interlayer Geogrid Reinforcement.

Emulsified asphalt, with a weight equivalent application rate of 0.45 liters/m^2 (~8 grams per sample surface area) was used as the interlayer tack coat (*32*). Although it is generally suggested to use the same asphalt-binder for the HMA as the tack coat, emulsified asphalt was intentionally selected and used in this study to simulate the worst-case scenario, as it is generally considered to be one of the weakest tack coat materials. Four hours cooling time period was allowed between compacting the bottom and top HMA lifts, respectively. Consistent with the standard PG 64-22 temperature requirements, the mixing and compaction temperatures for the HMA were 144 and 127 °C, respectively (*33*). Both the bottom and top 75-mm thick HMA lifts were compacted to a target density of 93±1%, i.e., 7±1% air voids (*33*). Density and air void (AV) determination were based on dimensional and volumetric computations within the target of 7±1% AV for both the control and geogrid reinforced HMA samples. Three HMA sample replicates were fabricated per geogrid type including the control.

Note that while 50 mm (or thinner) is the typical field HMA overlay thickness, 75 mm thick HMA lifts were adapted in this study (Table 3 and Figure 4) for the practical convenience of the laboratory test setup and protocol used as shown subsequently in Figure 5. Theoretically, 75 mm thickness was also considered to be conservative in terms of simulating the worst-case scenario for compaction (i.e., a thick lift will result in a slightly lower compaction density at the interface, and translating to a weaker bond). In future follow-up studies, however, it is strongly warranted to investigate typical HMA overlay thicknesses such as 50 mm and other thinner lifts like 25 mm thickness.

The Interlayer Shear-Bond Strength Test

As previously stated, there exist several test methods to evaluate the interlayer (interface) bonding of HMA layers including the PINE interface shear, Pull-off (tension), and torque-bond tests (*11-12, 20-21*). The PINE interface shear test, that has been proven to be a more practical and repeatable test, was used in this study (*12*). As shown in Figure 5a, the HMA sample is inserted with the bond interface oriented vertically. The PINE interface shear apparatus consists of two parts: namely, a ridged sleeve and a sliding sleeve. A ridged sleeve is used to hold one side of the test specimen rigidly and to provide a reaction force, while the sliding sleeve is used to hold the other side of the specimen that freely slides vertically perpendicular to the specimen's vertical axis and produces the shear load.

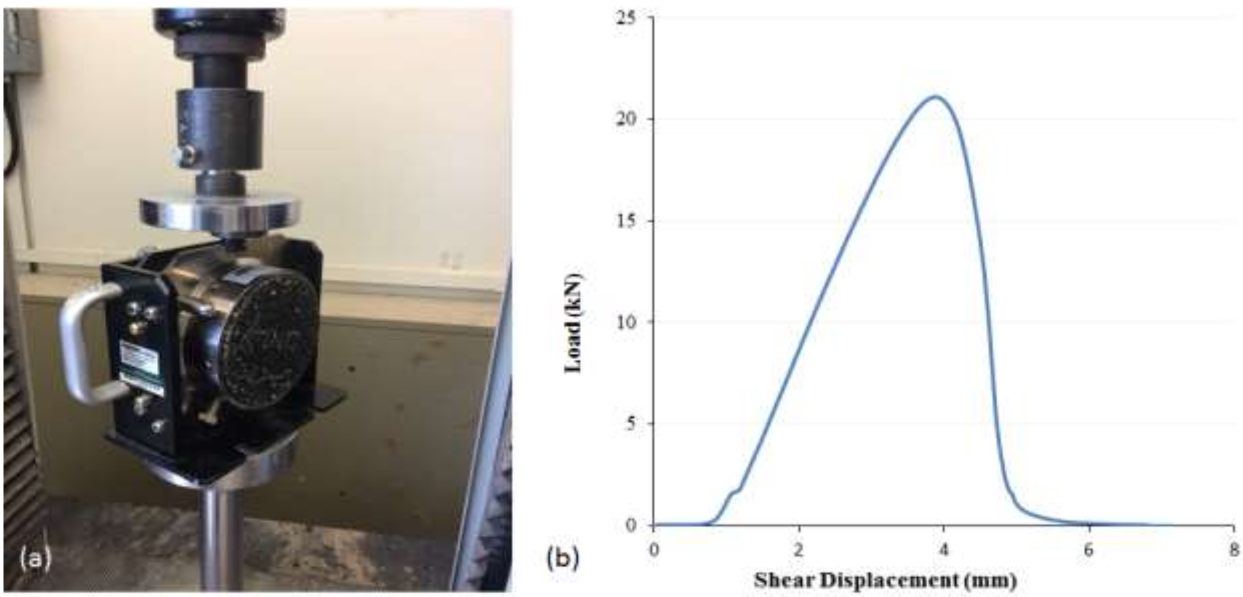

FIGURE 5 Shear Bond-Strength Test Setup (a) and Example Output Data (b).

In this study, the test was conducted at a monotonic loading rate of 5 mm/min at room temperature in accordance with the Texas standard test procedure Tex-249-F until sample failure (i.e., after the maximum load is achieved and the load has decreased substantially) (*33*). From the test data, a load-displacement (L-D) graph as exemplified in Figure 5b is generated and the peak load is used to determine the bond strength as illustrated in Equation 1 (*12*):

$$S_{max} = \frac{4P_{max}}{\pi D^2} \qquad \text{(Equation 1)}$$

In Equation 1, S_{max} is the maximum shear bond strength, P_{max} is peak (maximum) shear failure load, and D is the sample diameter, i.e., 150 mm in this study. After testing, the HMA samples would be sheared and split into the two HMA lifts as shown in Figure 6. Note that as illustrated in Equation 1 and the subsequently presented test results/analysis, this study was limited to primarily evaluating and quantifying the shear loading effects without consideration of the normal stresses on the tested samples.

FIGURE 6 Example HMA Sample Failure Mode (FA-50 Reinforced).

LABORATORY TEST RESULTS AND ANALYSIS

The failed HMA samples after testing and a plot of the average shear bond strength versus shear displacement are shown in Figures 7 and 8, respectively. All the HMA sample were tested after 5 days of molding to allow for curing and setting time of the emulsified asphalt so as to build ample bond strength. As theoretically expected, the control HMA samples without interlayer reinforcement exhibited the highest interlayer bond strength, averaging 747 kPa, and failed at the highest shear deformation of about 4.01 mm. The second-ranking in performance superiority was FA-30 at about 653 kPa. At a bond strength of about 225 kPa, FG-100 performed the poorest with the least shear displacement of about 2.55 mm.

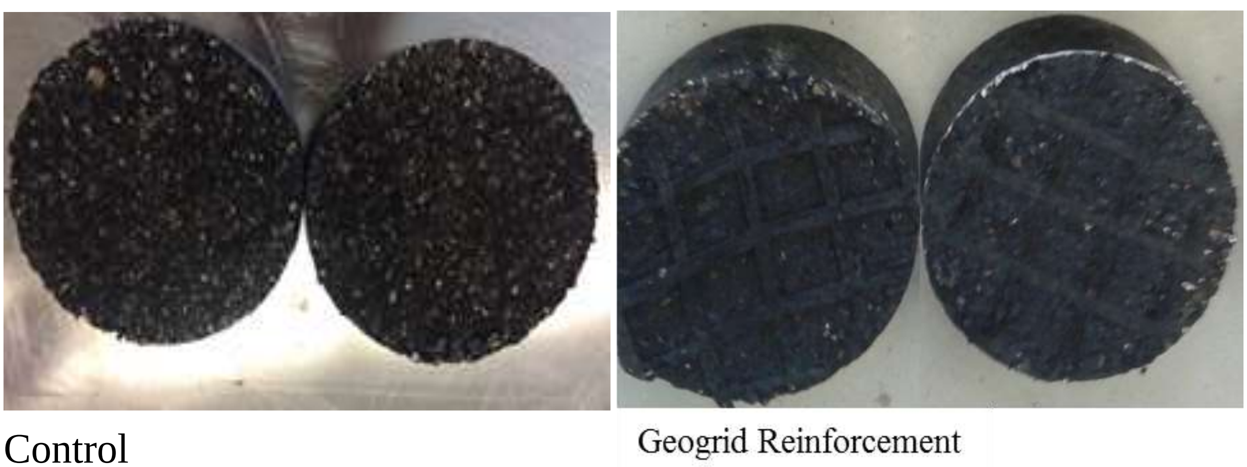

FIGURE 7 Example HMA Samples After Testing.

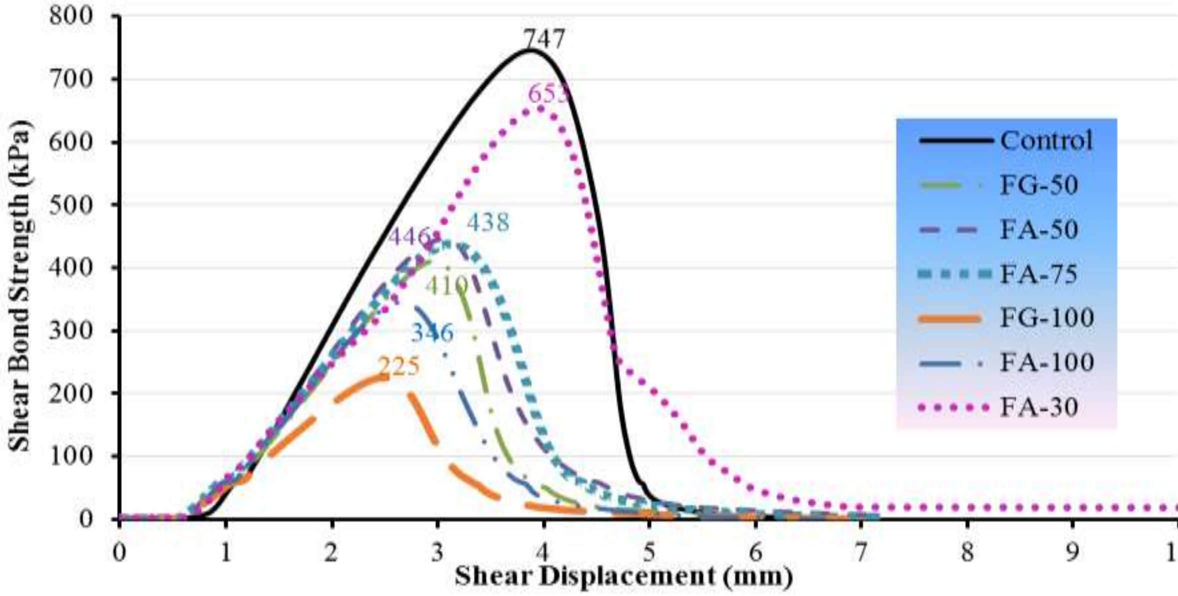

FIGURE 8 Interlayer Shear Bond Strength versus Displacement Plots.

Interlayer Shear-Bond Strength Results

Figure 8 shows that FA-50 and FA-75 are insignificantly different in terms of their interlayer bond strength performance and shear displacement failure. Furthermore, Figure 8 shows that the FA-50 and FA-75 grids offered superior shear bond strength over the tested FG grids. These results are distinctively evident in Figure 9 where the average (peak) interlayer bond strength is plotted as a function of the geogrid material grade in a bar chart. Figure 9 is also supplied with standard error bars that overlaps - indicating that only FA-30 is insignificantly different from the control. Statistically, if the error bars overlap, it means that the results/values are statistically insignificantly different.

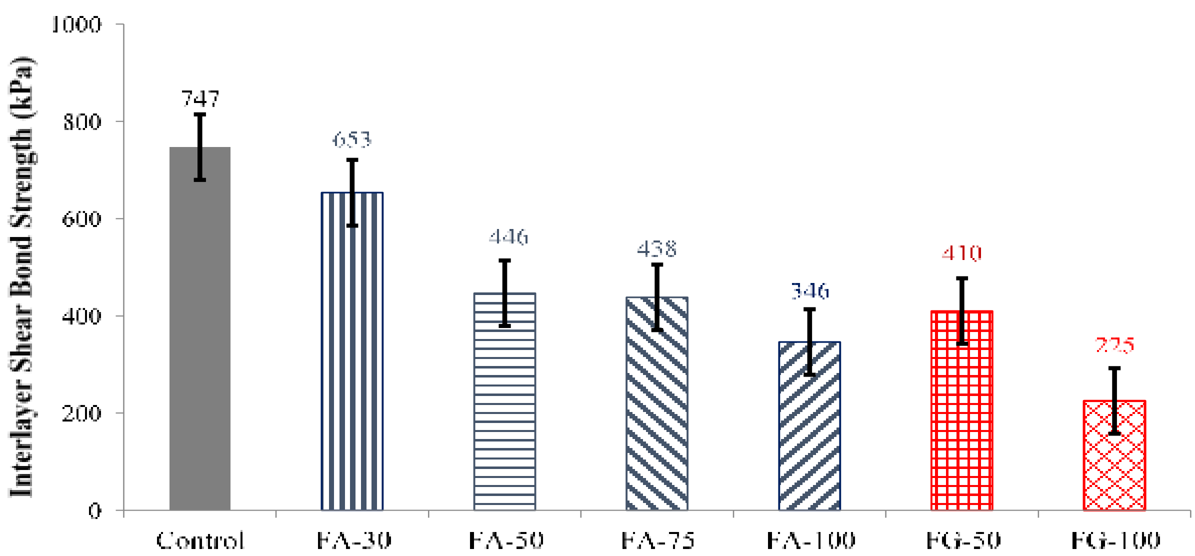

FIGURE 9 Interlayer Shear Bond Strength versus Geogrid Material Grade.

For the HMA mix evaluated and the test conditions considered, Figure 9 shows that FA (polyester-based) is superior to FG (fiberglass-based) in terms of the interlayer bond strength performance. That is, at all equivalent geogrid grades, the magnitude of the interlayer bond strength for the HMA samples reinforced with FA material was at least 1.1 times higher than those reinforced with FG material. By comparison, the interlayer bond strength of the control HMA samples is about 1.14 times better than the best geogrid performer (FA-30) and about 3.32 times better than the poorest performer (FG-100) in terms of the interlayer bond strength. Nonetheless, these measured bond strength values, ranging from 225 to 653 kPa, are insignificantly different from the values reported in the reviewed literature that range from 100 kPa to about 1500 kPa as shown in Table 1 for largely unreinforced HMA without any interlayer geogrid reinforcements.

When comparing FA-50 versus FA-75, it is evident in Figure 9 that the bond strength value of 446 kPa is hardly different from 438 kPa – theoretically suggesting that their in-service bonding strength performance would be insignificantly different. Thus, these two geogrid materials (FA-50 and FA-75) can be used in lieu of one another in as far as optimizing the interlayer bond strength is concerned. Furthermore, Figure 9 also shows a decay and loss in interlayer bond strength with an increase in the geogrid material grade. For instance, FA decreased from 653 kPa (Grade 30) to 346 kPa for Grade 100. Similarly, FG drastically declined by almost 50% from 410 kPa (Grade 50) to 225 kPa (Grade 100). Using the control as the reference datum, a reduction in the interlayer bond strength of as much as 69.9% due to the effects of interlayer reinforcement with FG-100 can be inferred from Figure 9. The least reduction in interlayer bond strength was computed for FA- 30 at 12.5%, i.e., 747 kPa to 653 kPa.

Test Data Variability and Statistical Analysis

The results plotted in Figures 8 and 9 represent an average of three replicates for both the control (unreinforced) and geogrid reinforced HMA samples, respectively. As shown in Table 4, the test was fairly repeatable with a coefficient of variation (COV) less than 30% - but with more data variability indicated for the FG reinforced samples based on its relatively higher COV values (*8*). One-way ANOVA and *t*-tests were also conducted at 95% confidence level (CL) to statistically quantify if the materials were statistically different and rank them accordingly (*34*). These statistical results are shown in Table 4.

TABLE 4 Data Variability and Statistical Analysis.

Material (Geogrid)	**COV (≤30%)**	**Is the Geogrid-interlayer performance Statistically Significantly different from the Control at 95% CL (α = 0.05)?**			**Statistical Ranking**
		Shear bond strength	*P-value*	Decision: Yes, if *P*<*α*	
Control	09.8%	(678, 857, 706; Avg = 747 kPa)	1.000	No (control)	A
FA-30	11.3%	(653, 586, 719; Avg = 653 kPa)	0.235	No	A
FA-50	14.7%	(441, 514, 383; Avg = 446 kPa)	0.011	Yes	B
FA-75	11.9%	(386, 490, 438; Avg = 438 kPa)	0.008	Yes	B
FA-100	15.6%	(381, 373, 284; Avg = 346 kPa)	0.003	Yes	B
FG-50	17.5%	(461, 442, 328; Avg = 410 kPa)	0.008	Yes	B
FG-100	19.0%	(247, 176, 253; Avg = 225 kPa)	0.001	Yes	C

Except for FA-30, Table 4 shows that all the geogrid reinforced samples are statistically different from the control (unreinforced) and that FA-50, FA-75, FA-100, and FG-50 are statistically indifferent and have the same statistical ranking. Therefore, either one of them can be used in lieu of the other in terms of bond strength – subject to meeting other performance requirements including their effectiveness in mitigating reflective cracking. Similarly, the results show that there is no major statistical difference between the "Control" and FA-30 reinforcement in as far interlayer bond strength performance is concerned. Statistically, the "Control" and FA-30 ranks at the top (at A) while FG-100 ranks at the bottom-most or poorest (at C). The rankings can also be traced to the standard error bars in Figure 9 that overlaps for the Groups A, B, and C, respectively, as shown in Table 4.

DISCUSSION AND SYNTHESIS OF THE FINDINGS

Interlayer (interface) bonding of the HMA pavement layers is very critical during construction, long-term performance, and durability, particularly where interlayer reinforcements such as geogrids are used (*12, 24*). This study has undoubtedly added valuable data/information to the pool of knowledge and literature on interlayer bond strength with respect to geogrid reinforcements in HMA. In particular, the study results have demonstrated that use of interlayer reinforcements in HMA has a profound effect on the interlayer bond strength and that due diligence must be cautiously exercised when selecting both the geogrid type and grade for use in HMA reinforcement to ensure optimum interlayer bonding.

Geogrid Material Comparison

Comparing the two geogrids evaluated, FA (polyester-based geogrid) outperformed FG (fiberglass-based) by over 10%, presumably due to the bitumen copolymer coating that contributed to its effective adhesiveness and bonding with the HMA and tack coat. This factor (bitumen copolymer coating) along with the relatively large mesh opening area and thin strands (Table 2) probably contributed to FA-30's statistically indifferent performance from the control (Table 4). The brittle characteristics of fiberglass may have contributed to FG's comparatively poor performance and relatively lower interlayer bond strength. By contrast, the flexibility characteristics of polyester enabled FA to properly embed itself into the rough HMA surface to form relatively strong interlayer bonds.

Effects of Geogrid Type and Grade

Both Figures 8 and 9 indicated reduction in the interlayer bond strength with the use of geogrid interlayer reinforcement, and, that both geogrid type and grade were influencing factors – with FG exhibiting more decay than FA. The loss in interlayer bond strength with increasing material grade for both the geogrids is partly attributed to the decreasing aperture (mesh opening) area and increasing strand dimensions (Table 2). This, in turn, decreases the HMA-tack-HMA contact/bonding area, as exemplified by the percentage HMA-HMA contact over a 150-mm diameter area. For the HMA mix and test conditions considered herein, FA material would be preferred over FG, with FA-30 that exhibited statistically indifferent performance from the control being recommended for optimum interlayer bond strength whilst simultaneously mitigating reflective cracking. Nonetheless, the measured interlayer bond strength values (ranging from 225 to 653 kPa) are comparable to the reviewed literature values (100-1500 kPa) of mostly unreinforced HMA shown in Table 1. Theoretically, this suggests that these geogrid interlayer reinforcement materials could be used with acceptable field bonding performance expectation – with FA (Grade 30) material being given preference over FG.

Simulating Field Conditions – New HMA over Field Core

To further supplement/validate the laboratory test results and simulate field conditions, 7.5-years old field cores were also used to evaluate the effects of the geogrid reinforcement (FA-30) on the interlayer bond strength. For this supplementary testing, only one geogrid type, namely FA-30, was demonstratively evaluated based on the assumption that the ranking/trend of the shear-bond strengths of field cores, under the same test conditions was theoretically not expected to be significantly different from that of the laboratory prepared specimens. Like the top HMA lift, the field cores (bottom lift) also comprised of 12.5-mm NMAS aggregates. As exemplified in Figure 10, a similar test configuration as listed in Table 3 was adapted albeit that the bottom 75-mm lift comprised of a field core and the top 75-mm lift a new HMA overlay.

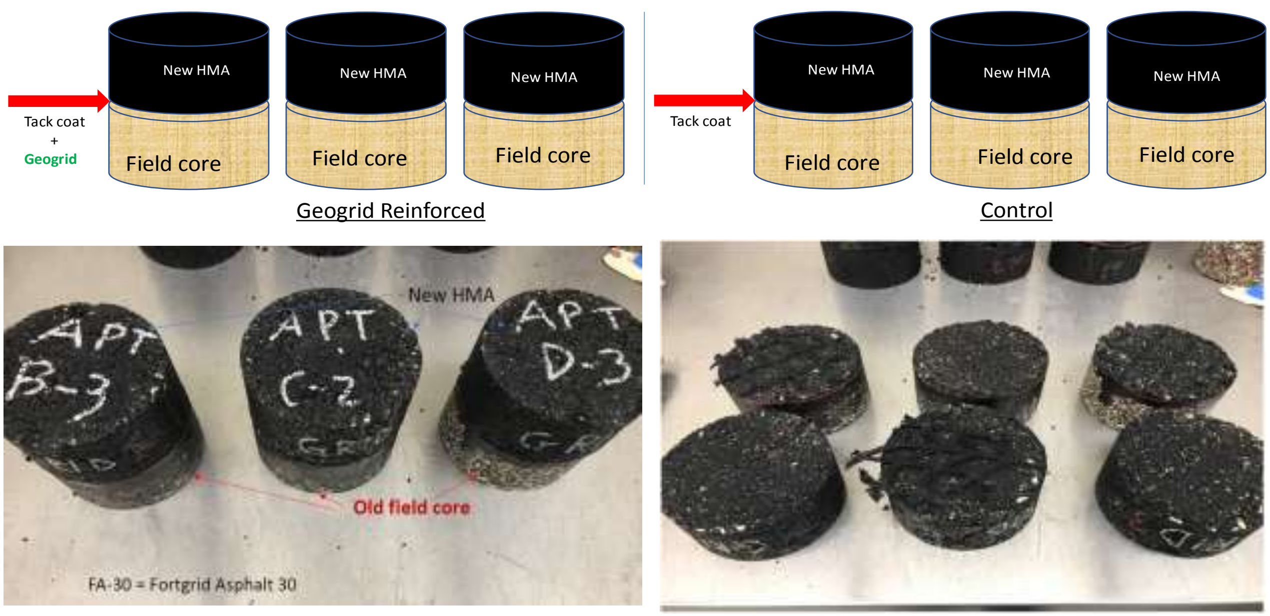

FIGURE 10 Test Configuration for New HMA Over Field Cores.

Three replicate tests were conducted for the “Control” and “FA-30” grid reinforcement, respectively; see Figure 10. Similar test conditions shown in Figure 5 were used. The test results are summarized in Table 5 and shows that the interlayer shear-bond strengths with the field core are statistically indifferent from those reported in Table 4 for both the “Control” and “FA-30” grid reinforcement, respectively. Similarly, “FA-30” and the “Control” are statistically indifferent. Considering that field cores simulating field conditions were used, these test results are plausible and to some degree validates the findings of this study. In addition, the calculated COV values were significantly less than 30% (Table 5) as was the case with the earlier test results reported in Table 4. This vindicates that the PINE interface shear test is repeatable with low data variability and statistically acceptable results.

TABLE 5 Shear-Bond Strength Results for New HMA Over Field Cores.

Parameter	Control	Geogrid Reinforcement (FA-30)
Test sample configuration	New HMA (75 mm thick) + tack coat + field core (75 mm thick)	New HMA (75 mm thick) + *grid (FA-30)* + tack coat + field core (75 mm thick)
Sample01	705 kPa	623 kPa
Sample02	738 kPa	608 kPa
Sample03	724 kPa	679 kPa
Average	722 kPa	637 kPa
COV (≤ 30%)	2.29%	5.88%
P-value	0.684 (> α =0.05)	0.735 (> α =0.05)
Statistical ranking	A	A

As stated above, the lab-sample and field-core results for the Control and FA, are statistically indifferent, slightly differing only by about 2.5%, i.e., 637 kPa (cores) versus 653 kPa (lab-samples). This is theoretically speculated to be due to similar controlled test conditions and sample preparation procedures as well as good workmanship. On the other hand, these findings could analytically infer that with proper construction practices and QC/QA protocols, interlayer bond strength close or equivalent to fresh HMA is attainable.

HMA Lift Thickness and Correlations to Field Conditions

Note that in both the lab-samples (Figure 4) and field-cores (Figure 10), 75 mm thickness was used (as opposed to the typical field 50 mm overlay thickness or less) for the practical convenience of the laboratory shear-bond test setup (Figure 5) as well as being conservative in terms of simulating the worst-case scenario for sample-edge compaction and bond strength. Therefore, future follow-up studies should focus on thinner HMA lifts including 50 and 25 mm thicknesses to comparatively assess their impacts on shear-bond strength results and supplement/substantiate the findings of this study. As this study only focused on the shear loading effects, another aspect worth investigating in future studies is the effects of the normal stresses on the shear behavior of the samples that was not considered in this study.

SUMMARY AND CONCLUSIONS

This laboratory study was conducted to comparatively evaluate and quantify the interlayer bond strength in HMA due to the effects of the geogrid reinforcements using unreinforced control HMA samples as the reference datum. Cylindrical HMA samples (150 mm diameter) gyratory compacted in two 75-mm lift thicknesses, with the geogrid reinforcement in-between the two lifts, were used for testing at room temperature under a monotonically shear loading rate of 5 mm/min. Emulsified asphalt was used as the interlayer tack coat and six different geogrid materials, polyester-based (FA) and fiberglass-based (FG), were comparatively evaluated. For the HMA mix and test conditions considered, the key findings and recommendations drawn from the study are summarized as follows:

- Structurally, the interlayer geogrid reinforcements are needed to enhance reflective crack mitigation in HMA overlays. However, as the study has shown, they may have an impact on the interlayer shear-bond strength and that the degree of impact is partly a function of the geogrid type/grade. For the geogrid materials evaluated in this study, the measured bond strength ranged from 225 to 653 kPa versus 747 kPa for the control (unreinforced) – which were all, nonetheless, satisfactorily comparable to the reviewed literature range of 100 to 1500 kPa for mostly unreinforced HMA.

- As theoretically expected, the unreinforced control HMA samples exhibited the highest interlayer bond strength closely followed by the FA (polyester) reinforcements, and lastly, FG (fiberglass).
- By comparison, FG-30 (polyester-based) was statistically indifferent from the control – substantiating that geogrid reinforcements while mitigating reflective cracking, can be satisfactorily used without any significant loss in the interlayer shear-bond strength provided that the right geogrid type/grade is used.
- FA geogrids out-performed FG by over 10% at all the material grades evaluated. HMA samples reinforced with FG exhibited the lowest interlayer bond strength, averaging about 57.5% lower than the control.
- Statistically, FA-50 performed indifferently from FA-75, FA-100, and FG-50 in terms of the interlayer shear-bond strength magnitude – thus, either one of them can be used in lieu of the other in as far as optimizing interlayer bond strength is concerned, subject to meeting other performance requirements including their effectiveness in mitigating reflective cracking.
- The simulation of field conditions using FA-30 and 7.5-years old field cores indicated that the interlayer shear-bond strengths of laboratory compacted HMA samples and the field cores did not differ significantly.

Overall, the study results have demonstrated that addition of interlayer reinforcements in HMA may have an impact on the interlayer shear-bond strength and that while interlayer reinforcement is structurally desired to mitigate reflective cracking in HMA overlays, due diligence must be cautiously exercised when selecting the geogrid type/grade to ensure sufficient interlayer bonding and minimize any potential delamination/debonding problems in service. Nonetheless, future follow-up studies should incorporate more field validation along with an array of HMA mixes and tack coat types for laboratory testing to substantiate these findings and to propose a standardized interlayer bond strength test procedure and screening criteria for geogrid reinforcement in HMA. Other aspects to consider in future follow-up studies should include thinner HMA lift-thicknesses (i.e., 50 mm, 25 mm, etc), using the same asphalt-binder as the HMA for the tack coat, testing more field cores with different geogrid types, and assessing the impacts of the normal stresses on the interlayer shear-bond strength.

ACKNOWLEDGEMENTS AND DISCLAIMER

The authors would like to thank Mr. Omar L. Torres**,** Mr. E. Abadi, and Geomatrix for their support and provision of the geogrid materials used in this study. The authors also acknowledge and thank Professor James W. Maina of the University of Pretoria, South Africa, for his technical contributions to the paper. Special thanks also go to all those who helped in the course of the study.

The contents of this paper reflect the views of the authors who are responsible for the facts and accuracy of the data presented herein and do not necessarily reflect the official views or policies of any agency or institute. This paper does not constitute a standard, specification, nor is it intended for design, construction, bidding, contracting, tendering, certification, or permit purposes. Trade names were used solely for information purposes and not for product endorsement, advertisement, or certification.

REFERENCES

1) Ali, K., Shahab, F., & Fereidoon, M. N. (2009). Effects of Geosynthetics on Reduction of Reflection Cracking in Asphalt Overlays. *Elsevier Journal of Geotextiles and Geomembranes*. Vol. 27 (1), PP 1–8.
2) AG (2013). Alliance Geosynthetics – Pavement Interlayer System. Technical Brochure, NILEX Civil Environmental Group, USA.
3) Cleveland, G.S., Button, J.W., & Lytton, R.L (2002). Geosynthetics in Flexible and Rigid Pavement Overlay Systems to Reduce Reflection Cracking. Research Report# FHWA/TX-02/1777. PP 1-297. Texas Department of Transportation (TxDOT) - RTI, TX, USA.
4) Thin Bituminous Surfacing Systems. Agrément South Africa (ASA).
5) Fyfe, G. (2011). Geotextile Reinforced Seals under Asphalt. Paper Publication. Geofabrics Australasia, Australia.
6) Mostafa, E., & Bandaru, R. (2011). Cost Effective Prevention of Reflective Cracking of Composite Pavement. Research Report FHWA/LA.11/478. LSU, Baton Rouge, USA.
7) TI (2015). Tensar International. GlasGrid Pavement Reinforcement System - The GlasGrid® System Extends Pavement Life Thus Reducing Maintenance and Life Cycle Costs. GlassGrid Brochure, USA.
8) Walubita, L.F., Faruk, A.N., Zhang, J., & Hu, X. (2015). Characterizing the Cracking and Fracture Properties of Geosynthetic Interlayer Reinforced HMA Samples using the Overlay Tester (OT). *Elsevier Journal of Construction and Building Materials*, Vol. 93, PP 695-702.
9) Geomatrix (2016). Geomatrix Product Website. Accessed September 2016.
10) Zornberg, J.G. (2011). Advances in the Use of Geosynthetics in Pavement Design. Conference Proceedings. Geosynthetics India'11, IIT Madras, Chennai, Sept 23-24, 2011.
11) Zaniewski, J.P., Knihtila, S.F., & Rashidi, H.N. (2015). Evaluation of the Bond Strength of Asphalt Overlay. Proceedings of International Airfield & Highway Pavements Conference 2015.
12) Wilson, B., Seo, A., & Sakhaeifar, M. (2013). Performance Evaluation and Specification of Trackless Tack. FHWA/TX-16/0-6814-1. Texas Transportation Institute, College Station, TX, 2013.
13) Johnson, E., Cruz, N., & Wood, T. (2015). Using the Florida Bond Test to Improve HMA Bond Strength and Durability – Technical Summary Report. MN, USA.
14) Mohammad, L., Elseifi, B., & Patel (2012). NCHRP Report# 712: Optimizing Tack Coat for HMA Placement. Washington DC – The National Academies Press.
15) Tran, N.H., Willis, R., & Julian, G. (2012). Refinement of the Bond Strength Procedure and Investigation of a Specification. NCAT Report# 12-04. Auburn, AL.
16) Solaimanian, M. (2013). Paving the Way. APA, Harrisburg, PA.
17) PI (2017). Pavement Interaction: http://www.pavementinteractive.org/article/de-bonding-of-hma-pavementslayer-bonding-2/ Accessed July 2017.

18) Gharaybeh et al. (2010). Evaluation of Bond Strength Between Old and New Pavement Overlays. Paper extract from Maters Thesis. JUST, Irbid, Jordan.
19) Vacin, O., Ponniah, J., & Tighe, S. (2002). Quantifying the Shear Strength at the Asphalt Interface. Technical Paper.
20) Denneman, E., Steyn, W.J.vdM., Visser, A.T., 2008. Guidelines for the Assessment and Certification of Thin Bituminous Surfacing Systems. Agrément South Africa (ASA).
21) White, G. (2015). Asphalt Overlay Bond Strength. Conference Proceeding - Airfield Pavement and Lighting Forum, At Sydney, New South Wales, Australia.
22) Wang, H., et al. (2015). HMA Pay Adjustment. Report# FHWA NJ-2015-007, Piscataway, NJ.
23) McGhee, K.K., & Clark, T (2009). Bond Expectations for Milled Surfaces and Typical Tack Coat Materials Used in Virginia. Research Report# 09-R21. VTRC, VA.
24) West, R.C., Zhang, J., & Moore, J. (2005). Evaluation of Bond Strength between Pavement Layers. NCAT Report 05-08. National Center for Asphalt Technology, Auburn, AL.
25) Brown, S.F., Thom, N.H., & Sanders, P.J. (2001). A study of grid reinforced asphalt to combat reflection cracking. *Journal of the Association of Asphalt Paving Technologists*. Vol. 90, pp 543-569.
26) Pasquini, E., Bocci, M., & Canestrari, F. (2014). Laboratory Characterisation of Optimized Geocomposites for Asphalt Pavement Reinforcement. *Geosynthetics International*. Vol. 21 (1), pp 24-36.
27) Safavizadeh, S.A. et al. (2015). Investigating Reflective Cracking Mechanisms in Grid-Reinforced Asphalt Specimens. *Journal of the Transportation Research Board*. TRR 2507, pp 29-38.
28) Saride, S., & Kumar, V.V. (2017). Influence of Geosynthetic-Interlayers on the Performance of Asphalt Overlays on Pre-Cracked Pavements. *Geotextiles and Geomembranes*. Vol 45(3), pp 184-196.
29) Kumar, V.V., Saride, S., & Peddinti, P.R.T. (2017). Interfacial Shear Properties of Geosynthetic Interlayered Asphalt Overlays. *Geotechnical Frontiers 2017*. March 12-17, Orlando, Florida, USA, GSP 277, 442-451.
30) Romeo, E., Freddi, F., & Montepara, A. 2013. Mechanical Behaviour of Surface Layer Fibreglass-Reinforced Flexible Pavements. *International Journal of Pavement Engineering*. Vol. 15 (2), pp 95-109.
31) Al-Qadi, I.L. et al. (2012). Best Practices for Implementation of Tack Coat: Part 2 – Field Study. Springfield, IL.
32) USDOT (2016). Tack Coat Best Practices. TechBrief FHWA-HIF-16-017. US Department of Transportation, Washington DC, USA.
33) TxDOT (2018). TxDOT– Texas Department of Transportation. Online Manuals and Test Procedures. Austin, TX, USA. Last accessed September 2018.
34) Ross, S.M. (2009). Introduction to Probability and Statistics for Engineers and Scientist – 4th Edition. UC – Berkeley, USA | Academic Press (AP) – Elsevier.